A New Liquid Membrane Technique for Gas Separation

A new liquid membrane separation technique for gas mixtures has been developed: feed and sweep gases flow through the lumen of two different sets of hydrophobic microporous hollow fibers while a liquid on the shell side acts as the membrane. This membrane is identified as the contained liquid membrane (CLM). Major shortcomings of immobilized liquid membrane techniques are eliminated. The novel separation device is identified as the hollow fiber contained liquid membrane (HFCLM) permeator. Experimental studies are made with different CO_2-N_2 feed mixtures and a pure helium sweep stream, with special emphasis on model landfill gas purification. Either pure water or an aqueous solution of K_2CO_3 is used as membrane. The effects of several variables on the performance of the HFCLM permeator have been studied. A three-component permeation model, incorporating axial pressure drop, is developed for binary mixture separation in a HFCLM permeator having a sweep gas stream. The experimental data show good agreement with the theoretical predictions.

Sudipto Majumdar,
Asim K. Guha,
Kamalesh K. Sirkar
Department of Chemistry
and Chemical Engineering
Stevens Institute of Technology
Hoboken, NJ 07030

Introduction

Polymeric membranes used for gas separation suffer in general from low values of selectivities and permeabilities (Matson et al., 1983; Sengupta and Sirkar, 1986). Liquid membranes, however, possess high species permeability and high selectivity. Very high values of the latter can be obtained if facilitated transport with suitable carrier species can be implemented (Bhave and Sirkar, 1986; Hughes et al., 1986; Jain and Schultz, 1982; Kimura et al., 1979; Kimura and Walmet, 1980; Leblanc et al., 1980; Matson et al., 1977; Meldon et al., 1986; Otto and Quinn, 1971; Smith and Quinn, 1980; Suchdeo and Schultz, 1974; Ward and Robb, 1967; Way et al., 1982).

Such liquid membranes are conventionally utilized as immobilized liquid membranes (ILM) (Ward, 1972). The liquid used as a membrane is immobilized in the pores of a microporous support, spontaneously wetted by the liquid. Thus aqueous electrolytic solutions are immobilized in hydrophilic microporous supports holding the liquid by capillary action.

This ILM technique and other variations, however, have major shortcomings. Renewal or replacement of the liquid membrane, if poisoned or otherwise, poses severe problems (Matson et al., 1983). Secondly, the criticality of humidity control in permeators with significant gas removal makes operation of a practical ILM system very difficult (Kimura and Walmet, 1980) if ILM flooding by condensation is to be avoided. In addition, existing ILM's for positive pressure difference (ΔP) applications employ a costly flat sandwiched configuration having a low membrane surface area per unit permeator volume. The study by Hughes et al. (1986) utilizing dense cellulose acetate hollow fibers suffered from very low flux levels and had to be operated with no positive ΔP.

A new hollow fiber contained liquid membrane (HFCLM) technique for gas separation is introduced here. Using the membrane liquid in the shell side between feed-gas-carrying and sweep-gas-carrying fibers, this technique bypasses the shortcomings of ILM techniques. We present the separation results for CO_2–N_2 mixtures in HFCLM permeators containing microporous hydrophobic hollow fibers. The extent of feed gas separation with helium as the sweep gas has primarily been studied, using water as the membrane; the facilitated transport separation results of an N_2–CO_2 mixture through a 30 wt. % aqueous K_2CO_3 solution will also be briefly indicated. A ternary permeation model has been developed to describe the observed separation behavior in the novel permeator provided with a sweep gas stream.

Most experiments were carried out with a 60% N_2–40% CO_2 gas mixture representing a typical landfill gas (60% CH_4–40% CO_2) since N_2 is a model replacement for CH_4. The permeabil-

Correspondence concerning this paper should be addressed to K. K. Sirkar.

ity of nitrogen and the separation factor for the CO_2–N_2 system in aqueous liquid membranes are quite similar to those for methane and the CO_2–CH_4 system. Thus, various CO_2—N_2 mixtures of this study simulated acid gas removal from hydrocarbons in general. The operating parameters were chosen to illustrate the process rather than to optimize the separation.

Hollow Fiber Contained Liquid Membrane Technique

Figure 1 shows a dense population of hydrophobic microporous hollow fibers of small outside diameter in a permeator shell. Water and aqueous electrolytic solutions do not penetrate the pores in these hydrophobic fibers unless the liquid pressure exceeds 10–15 atm.

In such a hollow-fiber assembly, the space between the adjacent fibers is filled with an aqueous liquid chosen to function as a liquid membrane. The hollow fibers identified by *F* in Figure 1 carry the high-pressure feed gas whereas those identified by *S* carry a sweep gas, usually at a pressure considerably lower than the feed pressure. Ideally, the fiber bundle should be arranged in such a way that a feed-gas-carrying fiber is immediately adjacent to a sweep-gas-carrying fiber. Since the fibers contain the aqueous liquid membrane, we identify this as a contained liquid membrane (CLM), as compared to an immobilized liquid membrane (ILM).

The feed gas species contact the membrane liquid at the pore mouths of the feed fiber outside surface. They dissolve at this feed gas-membrane liquid interface and diffuse through the liquid membrane to the open pores of the nearest sweep fiber, where they desorb. The desorbed gases are carried away through the sweep fiber lumina by an inert sweep gas. Otherwise the desorbed gases themselves generate the permeate gas stream flowing through the bore of *S* hollow fibers.

The aqueous liquid membrane, generally maintained at a pressure higher than the feed gas and permeate gas pressures, prevents physical mixing of the feed gas or the sweep (or permeate) gas. The aqueous liquid is introduced to the permeator shell side from a membrane liquid reservoir under pressure, Figure 2. The two sets of hollow fibers, tightly packed together in the permeator shell, provide a very high ratio of membrane surface area to volume. It is preferable to avoid the densest possible packing unless fibers with composite wetting characteristics are utilized, since fiber contact points without membrane liquid in between will allow mixing of the feed gas with the permeate gas.

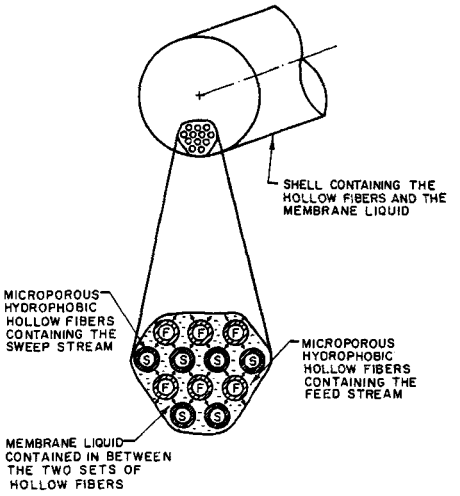

Figure 1. Configuration of hollow fiber contained liquid membrane (HFCLM).

The membrane liquid between the fibers is usually stationary. The shell port for discharging membrane liquid, Figure 2, may be used with a backpressure regulator to replace membrane liquid with fresh liquid. Otherwise this port is kept closed. For pure membrane liquid lost by evaporation into dry gas streams, there is an automatic and continuous supply of membrane liquid from the reservoir due to its higher pressure. Under such conditions the liquid would not be truly stationary. Such a hollow fiber contained liquid membrane (HFCLM) permeator has some distinct advantages:

1. Fiber wall defects lead only to a loss of membrane liquid through the fiber lumen. Unlike ILM systems and polymeric membrane permeators, feed does not leak into the permeate gas.
2. Gas humidification is unnecessary for a pure liquid.
3. The membrane is stable. Membrane liquid replenishment is easy.
4. The hollow fiber porosity and the pore tortuosity do not influence the gas flux in general.
5. Hydrophobic fibers prevent membrane flooding from moisture condensation in the fiber bore. Condensed moisture is mostly swept away by the gas stream.
6. The use of hollow fine fibers leads to a high membrane sur-

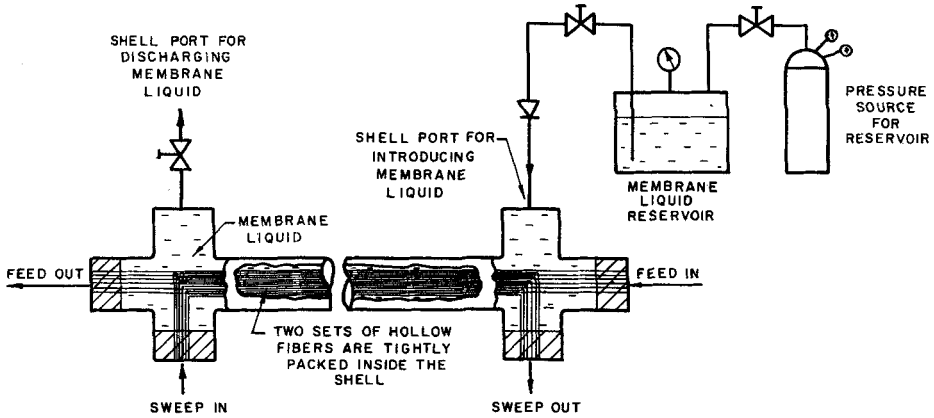

Figure 2. HFCLM permeator with membrane liquid reservoir and pressure source.

face area per unit permeator volume and low effective liquid membrane thickness.

7. The technique can be used with all four modes of permeate side operation: sweep gas, sweep liquid, vacuum, and conventional permeation (polymeric membranes). The sweep liquid with an aqueous liquid membrane can be either aqueous or organic. Aqueous sweep liquid will not enter the hollow fiber pores and contaminate the liquid membrane. Organic sweep liquid, if it wets the microporous support membrane, will do no harm as long as it is immiscible with the aqueous membrane.

Studies of permeation separation for other modes will be communicated elsewhere.

Theory

The following assumptions are used to analyze the gas permeation and separation of a binary feed gas mixture in an HFCLM permeator having a countercurrent sweep gas stream:

1. The feed and the sweep gas streams at any location consist of only three species, all being permeable
2. The permeability coefficient of each gas component is the same as that of the pure gas, and is independent of gas pressure (facilitated transport membranes with partial pressure-dependent permeability are considered later)
3. No mass transfer resistance exists in the gas phases
4. Diffusion along the gas flow path is insignificant compared to the bulk gas flow
5. A plug flow model can be used for both gas streams
6. The Hagen-Poiseuille equation governs fiber lumen pressure drop
7. The gas mixture viscosity is independent of pressure but depends on composition
8. The end effects inside the permeator are negligible
9. The deformation of the hollow fibers is negligible
10. Axial diffusion in the stationary membrane liquid is insignificant compared to the radial diffusion
11. The effect of a small movement of the membrane liquid (due to replenishment of membrane liquid lost by evaporation and/or leakage through defective fibers) on separation or pressure drop is negligible
12. An effective liquid membrane thickness, d, is assumed to exist along the permeator length as well as at all radial locations in the fiber bundle

A diagram of an HFCLM permeator having an effective liquid membrane thickness d is shown in Figure 3. Considering an equal number of feed and sweep fibers of identical dimensions in a permeator, the overall and component material balances between the feed inlet end of the permeator and any location at a distance l from the sweep inlet end can be written as

$$\text{Overall:}\quad L - V = L_f - V_f \tag{1a}$$

$$\text{CO}_2\text{:}\quad Lx - Vy = L_f x_f - V_f y_f \tag{1b}$$

$$\text{N}_2\text{:}\quad L(1 - x - u) - V(1 - y - v) = L_f(1 - x_f - u_f) - V_f(1 - y_f - v_f) \tag{1c}$$

$$\text{He:}\quad Lu - Vv = L_f u_f - V_f v_f \tag{1d}$$

Only three of the above equations are independent. If the treated feed gas end is the initial point for calculation ($l = 0$),

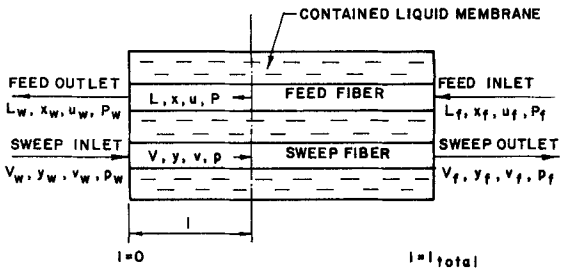

Figure 3. HFCLM permeator with countercurrent flow pattern.

the governing differential equations for permeation are

$$\text{CO}_2\text{:}\quad d(Vy)/dl = \pi D_o(Q_a/d)[Px - py] \tag{2}$$

$$\text{N}_2\text{:}\quad d[V(1 - y - v)]/dl = \pi D_o(Q_b/d)[P(1 - x - u) - p(1 - y - v)] \tag{3}$$

$$\text{He:}\quad d(Vv)/dl = \pi D_o(Q_c/d)[Pu - pv] \tag{4}$$

The differential equations governing the pressure drop in the two gas streams in the two sets of fiber lumina are

$$\text{Feed gas:}\quad dP/dl = 128RTL\mu_F/[\pi PD_i^4] \tag{5}$$

$$\text{Sweep gas:}\quad dp/dl = -128RTV\mu_S/[\pi pD_i^4] \tag{6}$$

Equations 2–4 along with Eqs. 1a–1d can be manipulated to yield six differential equations for each of the following dependent variables L, V, x, y, u, and v. Then, for each fiber set, we have one overall gas permeation equation, two species permeation equations, and one pressure drop equation. These equations constitute a set of eight nonlinear coupled ordinary differential equations (ODE) whose simultaneous solution subject to proper boundary and initial conditions will yield the profile of L, V, x, y, u, v, P, and p along the permeator. The boundary conditions for the ODE's are given by

$$l = 0 \Longrightarrow V = V_w;\quad y = 0(=y_w);\quad v = 1(=v_w) \tag{7}$$

$$l = l_t \Longrightarrow L = L_f;\quad x = x_f;\quad u = 0(=u_f);\quad P = P_f;\quad p = p_f \tag{8}$$

There are no published solutions for permeation separation with a sweep gas where the latter permeates to the feed and both streams encounter substantial pressure drop. Pan and Habgood (1974) analyzed binary mixture permeation in a flat membrane permeator with an impermeable sweep gas and no pressure drop in either gas stream. Stern and Leone (1980) treated the permeation separation of a quaternary mixture without any sweep gas or flow pressure drop. Further, although we have two sets of hollow fibers in the permeator, their function is radically different from multimembrane gas permeators studied by Perrin and Stern (1985, 1986) for binary separation and by Sengupta and Sirkar (1984, 1987) for ternary separations.

The set of eight coupled ODE's were solved numerically in dimensionless form (Majumdar, 1986) on a DEC 10 mainframe computer using standard IMSL subroutines. The complex

boundary-value problem of countercurrent ternary permeation with sweep flow and pressure drop in each stream was solved by using the IMSL routine DVCPR based on a finite-difference algorithm. The detailed solution procedure and computer program are available in Majumdar (1986).

Effective Liquid Membrane Thickness

To numerically solve the set of equations, the value of effective liquid membrane thickness d is necessary. There are three possible approaches. In one, assume various values of d and solve the system of equations. The value that brings the numerical results to closest agreement with experimental results is the effective d. Alternately, consider the volume of membrane liquid in a unit cell to exist around a feed fiber and determine its thickness. In the more rigorous third method, solve the diffusion equation in two dimensions in a unit cell to estimate the effective membrane thickness from the permeation rate and the permeability coefficient. We adopt the first two approaches here. The third method is studied elsewhere.

Of immediate interest is a simple geometrical method of determining the effective d. This value can be compared with the value of d that brings the numerical solution of the governing ODE's to the closest agreement with the observed permeator performance.

Figure 4a shows the cross section of the hollow fiber population in the permeator. The hollow fibers are assumed to be located on the circumference of hypothetical concentric circles. Assume further that only one kind of fibers (feed or sweep) exists along the circumference of a given concentric circle. If all the fibers are arranged in a triangular pitch, t, then

$$t = \{(D_b - D_o)/[12(n_f + n_s)]\} \cdot \{3\pi + \sqrt{[9\pi^2 + 24\sqrt{3}\pi(n_f + n_s)]}\} \quad (9)$$

Define D_e to be the equivalent diameter of a circle containing the liquid around any feed fiber in a unit cell; one way of defining the effective liquid membrane thickness d is

$$d = (D_e - D_o)/2 \quad (10)$$

Figures 4b and 4c indicate that there are two types of triangular cells, formed by two adjacent rows of feed and sweep fibers. They occur with equal frequency and remain next to each other in a fiber bundle. The corresponding equivalent diameters are

$$D_e = \sqrt{(3\sqrt{3}t^2/\pi - D_o^2/2)}$$
$$D_e = \sqrt{(6\sqrt{3}t^2/\pi - 2D_o^2)} \quad (11)$$

Two different values of membrane thickness are obtained for the two different configurations. However, the equivalent membrane thickness for triangular pitch can be calculated from Eq. 10 using the mean of the two D_e values.

The true cell in Figure 4a is a rhombus, shown in Figure 4d. To simplify, we replace the rhombus by a square, Figure 4e. The changed equations are (Majumdar, 1986)

$$t = \{(D_b - D_o)/[4(n_f + n_s)]\}\{\pi + \sqrt{[\pi^2 + 4\pi(n_f + n_s)]}\} \quad (12)$$

$$D_e = \sqrt{(8t^2/\pi - D_o^2)} \quad (13)$$

Using the above D_e, d can be determined from Eq. 10.

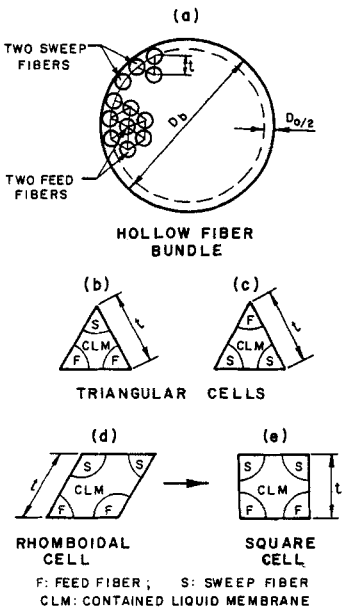

Figure 4. Unit cell configurations in a hollow-fiber bundle.

Experimental Method

The hydrophobic microporous hollow fibers used in this study were Celgard X-10 (Celanese Separations Products, Charlotte, NC) polypropylene fibers of 100 μm ID with 25 μm wall thickness. Their reported bubble point pressure is 1,034 kPa; their estimated mean pore size is 0.03 μm. The wall porosity is 20%.

A permeator was prepared using 600 such fibers in a 152.4 cm long, 1.27 cm dia. schedule 40 stainless steel (SS) 316 pipe, serving as the pressure vessel. The permeator fabrication consisted first of preparing a tight 600-fiber bundle with each bundle end being split into two separate bundles, each containing 300 fibers. To define D_b for the whole 600-fiber bundle, Figure 4, eight thin polyethylene (PE) tubes, each 19.68 cm long and 0.635 cm ID, were used as sleeves. These tubes, with 10–15 small holes on their surfaces, were sleeved over the fiber bundle to contain the fibers in a defined volume for two permeators, nos. 1 and 3. The whole assembly was inserted into the SS pipe. The two bundle ends, each containing 300 fibers, were taken out through two separate openings of a 1.27 cm cross-connector attached to the pipe. The third opening was used as the shell-side liquid inlet or outlet. Each fiber bundle end was potted in polyurethane (58:42 ratio of Polycin 1670 to Vorite 1701, Caschem Inc., Bayonne, NJ) and cured for seven days for full strength. The permeator was then pressure-tested with water for any leakage. For details, see the thesis by Majumdar (1986).

The fiber bundle for permeator 1 was assembled by preparing two separate mats each containing 300 fibers and placing one mat on top of the other. For permeators 3 and 4, only one mat of 300 feed fibers was prepared. Next, 300 sweep fibers were placed between feed fibers so that each sweep fiber remained next to a feed fiber. The mat was then rolled to prepare the bundle in each case (Majumdar, 1986).

In permeators 1 and 3 the membrane liquid contained between the pipe and the sleeves could communicate with the liquid inside the sleeves through the punched holes. Thus membrane liquid could be replaced radially as well as axially from one end of the bundle.

This radial liquid membrane replacement was eliminated in permeator 4 where a 0.61 cm ID and 1.03 cm OD Teflon pipe (Cole-Parmer, Chicago, IL) was inserted centrally in the 1.27 cm SS pipe. The annular gap between the SS and Teflon pipes was sealed by epoxy. The 600-fiber bundle was inserted through the Teflon pipe bore. Membrane liquid replacement could take place only axially from one permeator end. The fibers in the bundle were relatively free whether inside the PE sleeves or inside the Teflon pipe. We show a diagram of permeator 1 (or 3) in Figure 5.

The apparatus shown in Figure 6 had three components: feed line, sweep line, and membrane liquid line all tied to the HFCLM permeator, kept in an insulated water bath. The feed gas from a primary standard mixture cylinder (Matheson, E. Rutherford, NJ), was passed in succession through an oil filter, a feed humidifier, and an electronic flow controller (Matheson, model 8141-0452). The feed pressure at the permeator inlet was measured by a Heise pressure gauge (Dresser Industries, Newton, CT). A check valve before the permeator prevented accidental injection of membrane liquid into the flow controller.

The purified feed gas was passed successively through a test pressure gauge (Matheson) and an electronic flowmeter (Matheson, model 8141-0452). A liquid trap prevented carryover of droplets (from condensation or fiber leakage, or both) from fibers into the measuring instruments. Feed gas pressure was controlled by a Fairchild backpressure regulator (Epec Sales, Towaco, NJ). Gas compositions were determined by a Varian 3700 GC (gas chromatograph) containing a Porapak N 80/100 mesh column using He as the carrier gas. The instrumentation in the helium sweep gas line was essentially similar to that in the feed gas line.

A Matheson digital readout/control module (model 8249) was used to control the gas flow rates at the feed and sweep inlets and monitor flows through four transducers. The humidity and temperature of the two gas streams entering the permeator

BPR - BACK PRESSURE REGULATOR
BV - BALL VALVE
CPR - CYLINDER PRESSURE REGULATOR
CTB - CONSTANT TEMPERATURE BATH
CV - CHECK VALVE
FH - FEED HUMIDIFIER
FMC - FEED MIXTURE CYLINDER
FT - FLOW TRANSDUCER
FTC - FLOW TRANSDUCER CONTROLLER
GV - GATE VALVE
HTP - HUMIDITY/TEMPERATURE PROBE
LPGC - LIQUID PRESSURIZING GAS CYLINDER
LST - LIQUID STORAGE TANK
LT - LIQUID TRAP
MT - MOISTURE TRAP
OF - OIL FILTER
PG - PRESSURE GAUGE
RM - ROTAMETER
SGC - SWEEP GAS CYLINDER
SH - SWEEP HUMIDIFIER

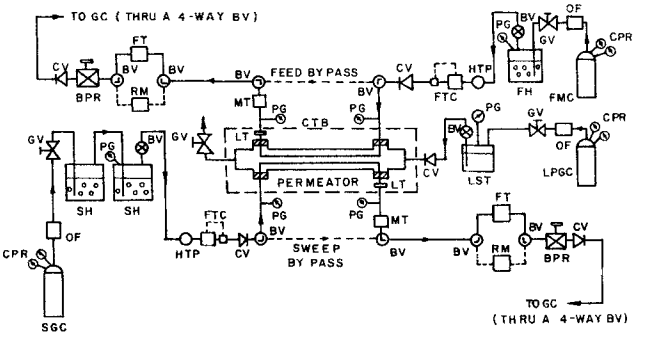

Figure 6. Purification loop.

were continuously displayed on a digital indicator (model HMI 32, Vaisala Inc., Woburn, MA).

The permeator shell-side inlet was connected to the membrane liquid storage tank, which was pressurized by a separate gas cylinder. The storage tank pressure, indicated by a Matheson test gauge, was always higher than that of the feed and sweep streams. The permeator shell-side outlet was opened only for draining membrane liquid.

The GC column was calibrated using a series of primary standard CO_2–N_2 gas mixtures. An average absolute area was calculated for each gas species. In an experimental run, the He content in the feed or sweep stream was determined by subtracting the combined CO_2–N_2 percentage from 100. This procedure was independently verified by injecting primary standard He–CO_2–N_2 mixtures into the GC.

For runs with humidified gas streams, the feed and sweep humidifiers were maintained at a higher pressure (~446 kPa) for at least three days. The membrane storage tank was also maintained at a pressure (~239.2 kPa) for 12 h to equilibrate

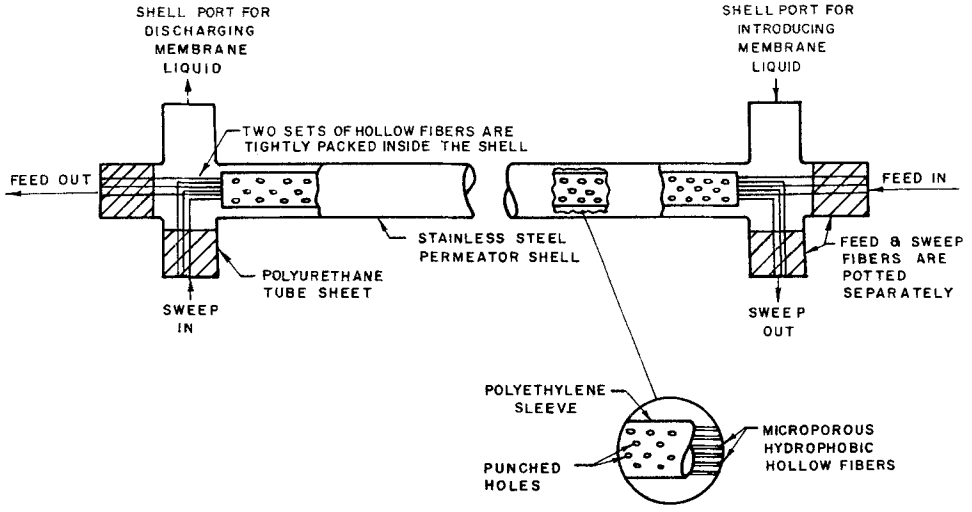

Figure 5. HFCLM permeator assembly with polyethylene sleeves, permeators 1 and 3.

the membrane liquid with the pressurizing gas, usually helium or the feed gas mixture. For each gas stream, flow rates and pressures at permeator inlets and outlets were measured along with incoming humidity, temperature, and outlet gas composition at 1 h intervals. Steady state was attained in 4–8 h.

Results and Discussion

All experiments utilized a feed gas mixture of 40% CO_2–60% N_2 at 25°C unless otherwise stated. The feed inlet and sweep outlet pressures were maintained at 411.5 kPa and 115.1 kPa respectively. The membrane liquid pressure was kept constant at 446 kPa except for the shell liquid pressure variation studies.

Estimation of pure-component gas permeabilities

The permeability of a gas species i through a pure water film Q_{iw}, may be estimated from the following product

$$Q_{iw} = D_{iw} \times H_{iw} \tag{14}$$

Table 1 summarizes the permeability values of CO_2, N_2, and He through pure water at different temperatures. The diffusivity and the solubility values were obtained from the references cited in Table 1.

Bhave and Sirkar (1987) have studied the permeation and separation behavior of CO_2–N_2 mixtures through fully exchanged Celgard 2400 ILM containing aqueous 30 wt. % K_2CO_3 solution. The permeability of N_2 for such a carbonate solution was found to be 2.28×10^{-15} mol · m/m² · s · Pa. The permeability of helium was estimated to be 3.98×10^{-15} mol · m/m² · s · Pa. The measured permeability of CO_2 through aqueous K_2CO_3 solution varied strongly with the applied partial pressure difference of CO_2 due to facilitated CO_2 transport. The existing theoretical models for CO_2 transport through aqueous electrolytic solutions (Otto and Quinn, 1971; Meldon et al., 1982; Jain and Schultz, 1982) were applied so far only to low carrier concentrations and at low partial pressures of CO_2. Table 2 shows that these models considerably underpredicted the observed CO_2–N_2 separation factor in 30 wt. % K_2CO_3 solution. Work is in progress to develop a better theoretical description. For the immediate objective of modeling the permeator behavior, the data of Bhave and Sirkar (1987) were correlated by the following equation

$$\alpha = 393.46 - 1{,}190.7(\gamma_1 x - \gamma_2 y) + 2{,}480.88(\gamma_1 x - \gamma_2 y)^2 - 2{,}432.75(\gamma_1 x - \gamma_2 y)^3 + 1{,}104.25(\gamma_1 x - \gamma_2 y)^4 - 188.27(\gamma_1 x - \gamma_2 y)^5 \tag{15}$$

where

$$\alpha = Q_a/Q_b; \quad \gamma_1 = P/P_{ref}; \quad \gamma_2 = p/P_{ref} \tag{16}$$

The facilitated CO_2 transport through a 30 wt. % K_2CO_3 solution is influenced by both diffusion and reaction rates (Kimura et al., 1979). Extensive studies of this effect are yet to be made. The experimental CO_2 permeability data of Bhave and Sirkar (1987) are valid for a membrane thickness of 0.0127 cm. Due to lack of any other data, the present results were considered to be valid for our case as long as the effective liquid membrane thickness was close to 0.0127 cm.

Table 1. Permeabilities of Pure Gases Through Water at Various Temperatures

Temp. °C	Gas	$D_{iw} \times 10^9$ m²/s	$H_{iw} \times 10^6$ mol/m³ · Pa	$Q_{iw} \times 10^{14}$ mol · m/m² · s · Pa
15	CO_2	1.4	445.73	62.40
	N_2	2.2	7.43	1.63
	He	6.2	4.35	2.69
25	CO_2	1.92	365.76	70.23
	N_2	3.0	6.22	1.86
	He	7.4	4.40	3.26
35	CO_2	2.4	261.69	62.81
	N_2	3.9	5.59	2.18
	He	8.4	4.48	3.76

D_{iw} data: CO_2, Thomas and Adams (1965); N_2, He, Wise and Houghton (1966).
H_{iw} data: Perry and Chilton (1973).

Table 2. Observed and Predicted CO_2-N_2 Separation Factor in 30 wt. % K_2CO_3 Solution at Various Partial Pressures of CO_2

Dimensionless* Partial Press. Difference of CO_2	Observed** Separ. Factor	Predicted† Separ. Factor	
		Model 1	Model 2
0.09193	303.11	183.46	180.38
0.22343	227.33	139.60	136.57
0.73868	174.46	99.91	96.81
1.12106	160.07	90.97	87.87
1.52184	138.99	85.35	82.16
1.91091	129.28	81.92	78.68

*Reference pressure: 101.325 kPa.
**Bhave and Sirkar (1987).
†Model 1: Otto and Quinn (1971).
Model 2: Jain and Schultz (1982); Meldon et al. (1982).

Estimation of liquid membrane thickness in HFCLM permeator

The fiber arrangement in one permeator would not be the same as that in another permeator; it would depend solely on the bundle preparation procedure if we disregard random variations for the time being. Therefore, a different arrangement of the fibers would lead to different liquid membrane thicknesses even though other physical parameters remained the same for all permeators. The geometrical method of determining d, valid only for the regular fiber arrangements, Figure 4, does not, however, predict different membrane thicknesses for different permeators. Calculations for a fiber bundle ($D_b = 0.635$ cm) containing 600 fibers (0.015 cm OD) yielded for the triangular arrangement a value of $d = 0.0108$ cm, and $d = 0.0095$ cm for the square arrangement.

The effective d was also determined by solving the three-component permeation model for several assumed values. The correct value of d should give a good agreement between calculated values and observed data. The effective membrane thicknesses for permeators 1 and 3, thus determined, were 0.01524 and 0.01115 cm, respectively. Since the fiber bundle for permeator 4 was also prepared in the same manner as for permeator 3, we assume the effective membrane thickness in permeator 4 to be also 0.01115 cm.

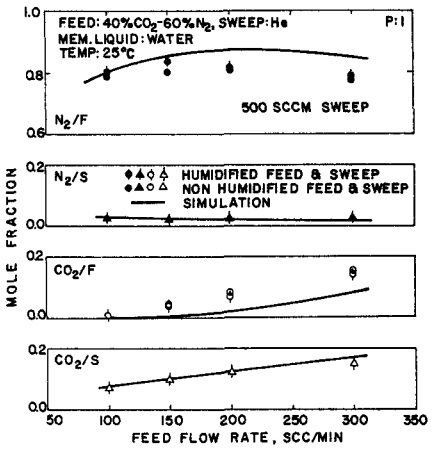

Figure 7. Feed flow variation studies in permeator 1.

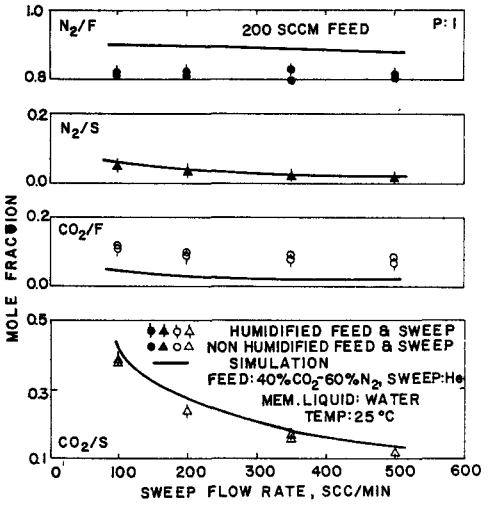

Figure 9. Sweep flow variation studies in permeator 1.

Model landfill gas purification: pure water liquid membrane

Purification studies with pure water liquid membrane were carried out with dry as well as completely humidified gas streams in two different permeators having different estimated d values. The data and the simulation results for feed gas flow variation are shown in Figure 7 for permeator 1 and Figure 8 for permeator 3; those for sweep flow variation are shown in Figure 9 for permeator 1 and Figure 10 for permeator 3. (In these and subsequent figures, gas compositions in feed and sweep outlet streams are identified by F and S, respectively. For example, N_2/F signifies N_2 mole fraction at the feed outlet and CO_2/S signifies CO_2 mole fraction at the sweep outlet.) Since the three-component permeation model does not distinguish between humidified and nonhumidified gas streams, the simulation results are applicable to both cases. Observe that at low and moderate feed flow rates, the treated gas had almost no CO_2 in it. As expected, the CO_2 content in the purified model landfill gas increased with an increase in feed flow rate, Figures 7 and 8. The same effect was also observed when the sweep flow rate decreased, Figures 9 and 10.

These performances suggest very little effect of the gas stream humidities on the separation. The minor effect, if any, can be attributed to a fourth component (moisture) present in the inlet gas streams (for humidified runs) and/or variation in room temperature affecting the inlet gas temperatures.

It is evident from Figures 7 and 8 (or Figures 9 and 10) that the separation performances of permeator 3 were better than those of permeator 1. For a given set of feed and sweep flow rates, the CO_2 content in the purified model landfill gas was significantly lower in permeator 3. Further, the sweep outlet N_2 content was higher. Since both permeators contained identical numbers and lengths of fibers, the better performance of permeator 3 was most likely due to a reduced liquid membrane thickness. Such a reduction in its effective d has more to do with the manner in which the two sets of fibers were put together in permeator 3.

In all four cases, the simulation results described the observed behavior quite well. For permeator 3 the agreement is better than that obtained in permeator 1. The model also predicted the pressure drop behavior of feed and sweep streams quite well.

Influence of feed gas composition

To determine the effect of feed composition, experiments were carried out with a 10% CO_2–90% N_2 feed gas mixture with

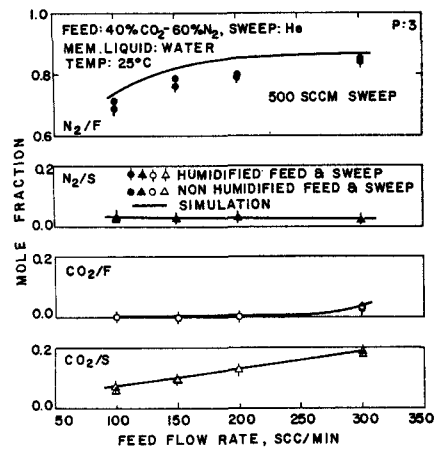

Figure 8. Feed flow variation studies in permeator 3.

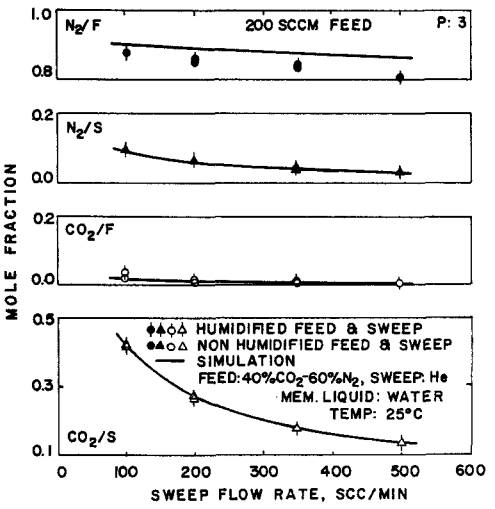

Figure 10. Sweep flow variation studies in permeator 3.

nonhumidified gas streams only. The feed flow and the sweep flow variation studies, shown in Figures 11 and 12 respectively, indicate a behavior generally similar to those presented earlier. A much smaller amount of CO_2 has to be removed here from the feed since it had much less CO_2. Therefore, the sweep outlet CO_2 content would be lower, as can be observed from its measured CO_2 content. The purified feed gas had very little CO_2 even at a high feed flow rate.

Figures 11 and 12 also indicate that the simulation results compare quite well with the experimental data. To test the applicability of the model further, experiments were done using a high CO_2 feed gas mixture (85.626% CO_2–14.374% N_2). The data and simulation results were in good agreement. Therefore, the three-component permeation model is valid over a wide range of feed compositions for pure liquid membranes without any chemical reactions.

Bath temperature variation

The results of separations carried out at four bath temperatures with dry feed and sweep streams are shown in Figure 13. Helium in the feed outlet increased with an increase in bath temperature. The CO_2 permeation rate remained more or less constant. Feed gas purification with respect to N_2 content improved considerably as the temperature was lowered.

Although species diffusion coefficient D_{iw} of gases in water increases with temperature, the solubility decreases. Due to these two opposing effects, the permeability value passes through a weak maximum. Table 1 shows such a behavior for CO_2. Since He diffusivity changes much more rapidly with temperature than does its solubility in water, the permeability increases monotonically for the experimental range of temperatures. So does the helium permeation rate. Table 1 also shows that N_2 permeability decreases with a decrease in temperature. At lower temperatures the N_2 permeation rate decreases. Therefore, the feed outlet shows an increase in N_2.

Shell-side pressure variation

Due to higher shell liquid pressure, the polypropylene hollow fibers in an HFCLM permeator are compressed. This deformation was neglected in the three-component permeation model.

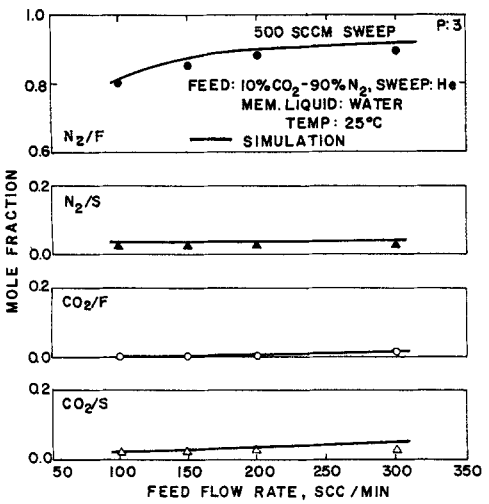

Figure 11. Effect of feed composition, feed flow variation studies.

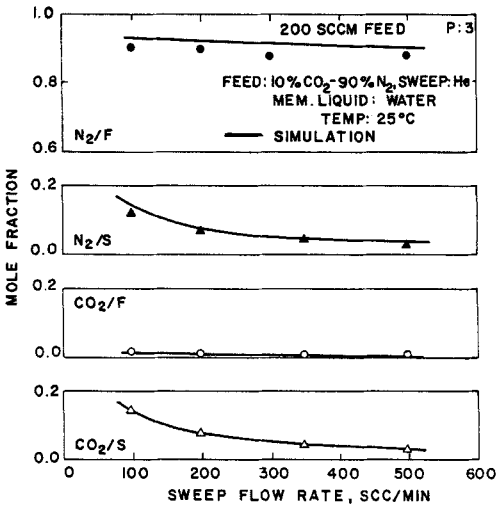

Figure 12. Effect of feed composition, sweep flow variation studies.

When pressurized externally, single hollow fibers undergo both radial and axial deformation (Stern et al., 1977; Thorman and Hwang, 1978): the fiber cross section decreases and fiber length increases. This should increase the gas stream pressure drop. We have observed such an increase in permeator 3 as the shell-side pressure increased from 411.5 to 515.0 kPa for dry gas streams at high flow rates.

The magnitude of the external pressure, however, did not have any significant effect on the permeation rate of CO_2 and N_2 for the following reason. Radial and axial deformations have opposite effects. The former reduces the gas permeation rate by cross-sectional area reduction whereas the latter increases the permeation rate by providing more permeation area (Stern et al., 1977). We have therefore neglected here the influence of the shell-side pressure, if any, on the permeation process. That the total pressure is constant along the liquid membrane thickness has also been ignored here.

Gas sources for pressurizing membrane liquid

A separate feed gas mixture cylinder was always utilized to pressurize the water membrane. To determine the effect of com-

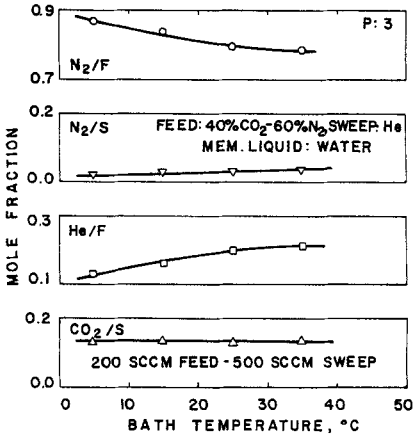

Figure 13. Effect of bath temperature variation on permeator performance.

position of this pressurizing gas on purification, the shell pressurizing gas cylinder (40% CO_2–60% N_2) was replaced by an He cylinder. We observed that the feed outlet helium content was essentially independent of the nature of the pressurizing gas. The sweep outlet CO_2 content in both cases also was almost the same. The results suggest that the membrane liquid within the permeator fiber bundle was locally in equilibrium with the feed and the sweep gas streams, and this phenomenon controlled the separation. The pressurizing gas, in equilibrium with the membrane liquid in the storage tank, does not affect the separation as long as the membrane liquid is free of any reactive species.

Stability of HFCLM

Some of the data reported earlier were obtained by operating the system continuously for as long as four days at a stretch, without any difficulty. This demonstrates that such a liquid membrane based process is very stable. The experimental data mentioned above were taken at various feed and sweep flow rates. The results for one experimental run, continued for over 24 h, are shown in Figure 14. This particular experiment was carried out at a feed inlet pressure of 377.1 kPa. Although the gas streams introduced were dry, a stable permeator performance was achieved, as shown. Without the continuous and automatic regeneration of liquid membrane from reservoir, such conditions would lead to instability and a quick disappearance of the membrane altogether. This is a major distinction between the present and earlier liquid membrane techniques. It is obvious that the HFCLM permeator can be used for long-term runs when a pure liquid is used as the membrane.

Model landfill gas purification: aqueous 30 wt. % K_2CO_3

Although pure water has separation characteristics comparable to or somewhat better than synthetic polymeric membranes commercially utilized for CO_2–CH_4 separation, its selectivity is not very high. To increase the selectivity as well as recovery, aqueous 30 wt. % K_2CO_3 solution was also used as a liquid membrane with both incoming gas streams being completely humidified to prevent localized drying or precipitation of salt. However, humidity control inside the permeator is not required.

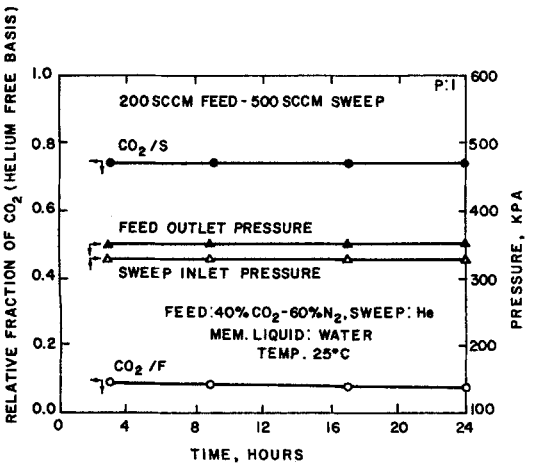

Figure 14. Stability of contained liquid membrane.

Condensed moisture in hydrophobic fiber bores would not lead to membrane flooding.

Separation experiments with K_2CO_3 solution as a liquid membrane were carried out in permeator 4. Unlike permeators 1 and 3, permeator 4 does not have an extra shell space around the fiber bundle. This drastically reduces the membrane liquid inventory in the permeator. The membrane liquid was pressurized by a pure He gas cylinder. An essentially steady gas composition was achieved within 6 h. The treated gas had almost no CO_2 in it and 90% of the feed N_2 was recovered during purification. However, sweep-side pressure increased slowly due to minute leakages of highly viscous membrane liquid into the sweep fibers. The results demonstrated that highly efficient purification and recovery of model landfill gas is possible using aqueous 30 wt. % K_2CO_3 solution as a liquid membrane.

In the above experiment, the sweep gas stream was introduced through the fiber set undergoing a 90° bend at the permeator ends, whereas the feed stream was introduced through the straight set of fibers. The sharp bends in the fibers might have caused some defects and membrane liquid leakage. Therefore, in the next experiment the feed gas was introduced through the fiber set with bends and the sweep stream was introduced through the straight fibers. Since the pressure difference between the shell liquid and the feed stream was very low, it was expected that the extent of membrane liquid leakage to the feed fibers, if any, would be very small.

With this arrangement, a stable and excellent performance of permeator 4 was achieved. Results of purification studies carried out at two different feed flow rates, as well as results of numerical simulations, are plotted in Figure 15. The general conclusions are similar to those obtained with pure water as the liquid membrane except that much higher purification was achieved. The sweep outlet N_2 composition is less than 5%, showing a higher recovery of N_2 in this case. As expected, the CO_2 percentage in the treated gas as well as in the sweep outlet stream increased with an increase in feed flow rate.

Although the numerical model for a reactive liquid membrane is an empirical one, the results appeared to describe the observed behavior fairly well. However, prediction of gas compositions at the feed outlet needs improvement.

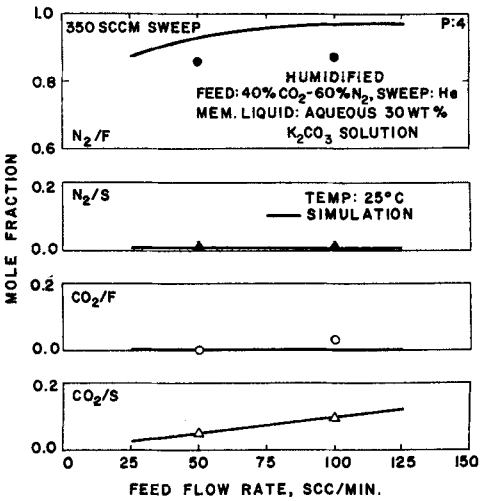

Figure 15. Permeator performances with aqueous potassium carbonate solution as membrane liquid.

Comparison of HFCLM with Other Membrane and Membrane-Based Processes

The permeation rates and separation factors of the liquid membrane systems are compared now with those of polymeric membrane systems used for CO_2 separation. Monsanto's Prism separator, which uses polysulfone membrane, has the following value for CO_2 permeation rate (Kulkarni et al., 1983): $[Q_a/d]|_{\text{polysulfone}} = 1.4 \times 10^{-8}$ mol/m$^2 \cdot$ s $\cdot$ Pa, the separation factor for the CO_2–N_2 system being around 38.

For $d = 0.01115$ cm in permeator 3, the CO_2 permeation rate through pure water is $[Q_a/d]|_{\text{water}} = 0.63 \times 10^{-8}$ mol/m$^2 \cdot$ s $\cdot$ Pa. The separation factor for the CO_2–N_2 system through pure water is about 37.7. Thus, the CO_2 permeation rate through pure water in the HFCLM permeator is marginally lower than that of commercial polymeric membranes while the separation factor is comparable. Using smaller hollow fibers, membrane thickness d could be reduced two to three times and the liquid membrane permeation rate would be comparable to or higher than that of polysulfone membrane.

With aqueous 30 wt. % K_2CO_3 solution as liquid membrane, the overall permeation rate of CO_2 for the given HFCLM permeator was estimated to be $[Q_a/d]|_{\text{overall}} = 0.37 \times 10^{-8}$ mol/m$^2 \cdot$ s $\cdot$ Pa; the overall separation factor for the CO_2–N_2 system was calculated to be 180. The prism process uses two permeation stages and high recycle to produce a CH_4 recovery of 81% (Early et al., 1983; Hilliard and Kilgour, 1983). With the present single-stage liquid membrane system, 80% N_2 was recovered when pure water was used as the liquid membrane and about 95% N_2 was recovered when aqueous carbonate solution was used. Note that the amount of CH_4 yield in such a permeator would be somewhat less than that of N_2 due to a higher permeability of CH_4 in water and aqueous carbonate solution. Still, extremely high recovery of methane is possible without any recycle (the results will be reported elsewhere). This will lead to a substantial saving in compression energy. In addition, the amount of feed gas to be processed, for a given amount of methane product, will be considerably less. Note further that the permeation rate of CO_2 through carbonate solution can be considerably increased by incorporating a suitable catalyst for CO_2 hydrolysis, such as TeO_3^- or AsO_2^- (Kimura et al., 1979).

In an HFCLM permeator, it is conceivable to have contact points between a feed fiber and a sweep fiber without any membrane liquid in between. This would be equivalent to a defect in a polymeric membrane. However, since the membrane liquid is always at a higher pressure, such a situation is highly unlikely. In fact, we have never encountered this in our experimental studies. To prevent such a situation from happening, one can have hollow fibers with composite wetting characteristics: the outside surface hydrophilic and the rest hydrophobic. This will ensure an immobilized aqueous liquid membrane in the fiber pores even at feed and sweep fiber contact points without any shell-side membrane liquid.

Qi and Cussler (1985) have recently suggested using hydrophobic microporous hollow-fiber modules for gas absorption. One can use two such modules for gas separation, one in sorption mode and the other in desorption mode. Using the Yang and Cussler (1986) correlation for water flowing outside the hollow fibers in parallel flow, the mass transfer coefficient for CO_2 in the dense packed module (external void fraction 0.6) is calculated to be 3.07×10^{-4} cm/s. In the present study, the mass transfer coefficient for CO_2 in permeator 3 (external void fraction 0.66) is obtained as 1.72×10^{-3} cm/s. Thus, an HFCLM permeator with stationary liquid has a mass transfer advantage. This is possibly due to the following. In a well-packed hollow fine fiber contacting module, there is considerable channeling in the shell-side liquid when operated in a contacting mode (Yang and Cussler, 1986). Further, the contiguous sweep fibers in an HFCLM are likely to result in a sharper concentration profile than in a simple contactor that is either absorbing or desorbing a gas. However, a more detailed comparison would be necessary to evaluate the utility of either concept in an economic framework that includes the cost of absorbent, modules and pumps.

Acknowledgment

The financial support of the New York State Energy Research and Development Authority and the New York Gas Group is gratefully acknowledged. The authors are also grateful to G. E. Walmet for useful discussions and to A. Sengupta and R. R. Bhave for their contributions. We thank Celanese Separations Products, Charlotte, NC for generously supplying us with Celgard hollow fibers.

Notation

d = liquid membrane thickness
D_b = hollow fiber bundle diameter
D_e = equivalent diameter of a circle enclosing liquid membrane around any feed fiber
D_i, D_o = inside, outside diameters of microporous hollow fibers
D_{iw} = species i diffusion coefficient in pure water
H_{iw} = solubility of gas species i in pure water
l = distance of any permeator location, starting from sweep inlet end
l_t = total length of permeation in a permeator equal to l_{total}
L, L_f, L_w = feed-side gas flow rate per fiber at any location, at feed inlet end, at feed outlet end of permeator
n_f, n_s = total number of feed fibers or sweep fibers in a bundle
p, p_f, p_w = sweep-side pressure at any location, at sweep outlet end, at sweep inlet end of permeator
P, P_f, P_w = feed-side pressure at any location, at feed inlet end, at feed outlet end of permeator
P_{ref} = reference pressure
Q_a, Q_b, Q_c = permeability of carbon dioxide, nitrogen, helium
Q_{iw} = permeability of gas species i in pure water
R = universal gas constant
t = distance between the centers of two adjacent fibers in a fiber bundle
T = absolute temperature
u, u_f, u_w = mole fraction of helium in feed-side gas mixture at any location, at feed inlet end, at feed outlet end of permeator
v, v_f, v_w = mole fraction of helium in sweep-side gas mixture at any location, at sweep outlet end, at sweep inlet end of permeator
V, V_f, V_w = sweep-side gas flow rate per fiber at any location, at sweep outlet end, at sweep inlet end of permeator
x, x_f, x_w = mole fraction of carbon dioxide in feed-side gas mixture at any location, at feed inlet end, at feed outlet end of permeator
y, y_f, y_w = mole fraction of carbon dioxide in sweep-side gas mixture at any location, at sweep outlet end, at sweep inlet end of permeator

Greek letters

α = ideal separation factor, Eq. 16
γ_1, γ_2 = dimensionless feed pressure, sweep pressure, Eq. 16
μ_F, μ_S = viscosity of feed-side gas mixture, sweep-side gas mixture at any location of permeator
π = 3.14159 . . .

Literature Cited

Bhave, R. R., and K. K. Sirkar, "Gas Permeation and Separation by Aqueous Membranes Immobilized Across the Whole Thickness or in

a Thin Section of Hydrophobic Microporous Celgard Films," *J. Membrane Sci.*, **27**, 41 (1986).
———, "Gas Permeation and Separation with Aqueous K_2CO_3 Membranes Immobilized Across the Whole Thickness or in a Thin Section of Hydrophobic Microporous Films and Hollow Fibers," Manuscript (1987).
Early, C. L., R. L. Kilgour, and S. S. Medvetz, "Monsanto Prism Separators for Upgrading Landfill Gas," Government Refuse Collection and Disposal Ass. Meet., Winnipeg, Manitoba, Canada (Aug.–Sept., 1983).
Hilliard, J. M., and R. L. Kilgour, "Landfill Gas Upgrading with Monsanto Prism Separators at Florence, Alabama," Government Refuse Collection and Disposal Ass. Meet., Winnipeg, Manitoba, Canada (Aug.–Sept., 1983).
Hughes, R. D., J. A. Mahoney, and E. F. Steigelmann, "Olefin Separation by Facilitated Transport Membranes," *Recent Developments in Separation Science*, N. N. Li, J. M. Calo, eds., CRC Press, Boca Raton, FL, **9**, 173 (1986).
Jain, R., and J. S. Schultz, "A Numerical Technique for Solving Carrier-Mediated Transport Problems," *J. Membrane Sci.*, **11**, 79 (1982).
Kimura, S. G., S. L. Matson, and W. J. Ward, "Industrial Applications of Facilitated Transport," *Recent Developments in Separation Science*, N. N. Li, ed., CRC Press, West Palm Beach, FL **5**, 11 (1979).
Kimura, S. G., and G. F. Walmet, "Fuel Gas Purification with Permselective Membranes," *Sep. Sci. Technol.*, **15**, 1115 (1980).
Kulkarni, S. S., E. W. Funk, N. N. Li, and R. L. Riley, "Membrane Separation Processes for Acid Gases," *AIChE Symp. Ser.*, **79** (229), 172 (1983).
LeBlanc, O. H., W. J. Ward III, S. L. Matson, and S. G. Kimura, "Facilitated Transport in Ion Exchange Membranes," *J. Membrane Sci.*, **6**, 229 (1980).
Majumdar, S., "A New Liquid Membrane Technique for Gas Separation," Ph.D. Diss. Dept. Chemistry Chem. Eng., Stevens Inst. Technol., Hoboken, NJ (1986).
Matson, S. L., C. S. Herrick, and W. J. Ward, "Progress on the Selective Removal of H_2S from Gasified Coal Using an Immobilized Liquid Membrane," *Ind. Eng. Chem. Process. Des. Dev.*, **16**, 370 (1977).
Matson, S. L., J. Lopez, and J. A. Quinn, "Separation of Gases with Synthetic Membranes," *Chem. Eng. Sci.*, **38**, 503 (1983).
Meldon, J. H., P. Stroeve, and C. E. Gregoire, "Facilitated Transport of Carbon Dioxide: A Review," *Chem. Eng. Commun.*, **16**, 263 (1982).
Meldon, J., A Paboojian, and G. Rajangam, "Selective CO_2 Permeation in Immobilized Liquid Membranes," *Industrial Membrane Processes*, R. E. White, P. N. Pintauro, eds., *AIChE Symp. Ser.* **82** (248), 114 (1986).
Otto, N. C., and J. A. Quinn, "The Facilitated Transport of Carbon Dioxide Through Bicarbonate Solutions," *Chem. Eng. Sci.*, **26**, 949 (1971).
Pan, C. Y., and H. W. Habgood, "An Analysis of Single-Stage Gaseous Permeation Process," *Ind. Eng. Chem. Fundam.*, **13**, 323 (1974).
Perrin, J. E., and S. A. Stern, "Modeling of Permeators with Two Different Types of membranes," *AIChE J.*, **31**, 1167 (1985).
———, "Separation of a Helium-Methane Mixture in Permeators with Two Types of Polymer Membranes," *AIChE J.*, **32**, 1889 (1986).
Perry, R. H., and C. H. Chilton, eds., *Chemical Engineers' Handbook*, 5th ed., McGraw-Hill, New York, p. 3–224 (1973).
Qi, Z., and E. L. Cussler, "Microporous Hollow Fibers for Gas Absorption," *J. Membrane Sci.*, **23**, 321 (1985).
Sengupta, A., and K. K. Sirkar, "Multicomponent Gas Separation by an Asymmetric Permeator Containing Two Different Membranes," *J. Membrane Sci.*, **21**, 73 (1984).
———, "Membrane Gas Separation," *Progress in Filtration and Separation*, R. J. Wakeman, ed., Elsevier, Amsterdam, **4**, 289 (1986).
———, "Ternary Gas Mixture Separation in Two-Membrane Permeators," *AIChE J.*, **33**, 529 (1987).
Smith, D. R., and J. A. Quinn, "The Facilitated Transport of Carbon Monoxide Through Cuprous Chloride Solutions," *AIChE J.*, **26**, 112 (1980).
Stern, S. A., and S. M. Leone, "Separation of Krypton and Xenon by Selective Permeation," *AIChE J.*, **26**, 881 (1980).
Stern, S. A., F. J. Onorato, and C. Libove, "The Permeability of Gases Through Hollow Silicone Rubber Fibers: Effect of Fiber Elasticity on Gas Permeability," *AIChE J.*, **23**, 567 (1977).
Suchdeo, S. R., and J. S. Schultz, "The Permeability of Gases Through Reacting Solutions: The Carbon Dioxide-Bicarbonate Membrane System," *Chem. Eng. Sci.*, **29**, 13 (1974).
Thomas, W. J., and M. J. Adams, "Measurements of Diffusion Coefficients of Carbon Dioxide and Nitrous Oxide in Water and Aqueous Solutions of Glycerol," *Trans. Faraday Soc.*, **61**, 668 (1965).
Thorman, J. M., and S. T. Hwang, "Compressible Flow in Permeable Capillaries Under Deformation," *Chem. Eng. Sci.*, **33**, 15 (1978).
Ward, W. J., "Immobilized Liquid Membranes," *Recent Developments in Separation Science*, N. N. Li, ed., CRC Press, Cleveland, **1**, 153 (1972).
Ward, W. J., and W. L. Robb, "Carbon Dioxide-Oxygen Separation: Facilitated Transport of Carbon Dioxide Across a Liquid Film," *Science*, **156**, 1481 (1967).
Way, J. D., R. D. Noble, T. M. Flynn, and E. D. Sloan, "Liquid Membrane Transport: A Survey," *J. Membrane Sci.*, **12**, 239 (1982).
Wise, D. L., and G. Houghton, "The Diffusion Coefficients of Ten Slightly Soluble Gases in Water at 10–60°C," *Chem. Eng. Sci.*, **21**, 999 (1966).
Yang, M. C., and E. L. Cussler, "Designing Hollow-Fiber Contactors," *AIChE J.*, **32**, 1910 (1986).

Manuscript received Jan. 21, 1987, and revision received Feb. 16, 1988.